Macromolecular Chemistry and Physics
www.mcp-journal.de

Check for updates

Reversible Hydrogels with Switchable Diffusive Permeability

*Paola Nicolella, Daniel Lauxen, Mostafa Ahmadi, and Sebastian Seiffert**

Hydrogels are polymer networks swollen in water that are characterized by soft mechanics and high permeability. This makes them good candidates for separation and membrane technologies. The diffusion is controlled by the mesh size of the network, and this can be made tunable through the introduction of thermoresponsive polymers. However, this is still a developing field. To contribute to this development, a dual dynamic network is formed composed of four-arm polyethylene glycol precursors in which each arm is functionalized with both a terpyridine moiety capable of forming reversible metal–ligand complexes along with branches of poly(*N*-isopropylacrylamide) (pNIPAAm), which can be switched between expanded and collapsed states and therewith offers a path for switching the microscopic gel-network mesh size, along with the macroscopic gel elasticity. The dually sensitive hydrogel has the capability of doubling its elastic modulus when going above the lower critical solution temperature (LCST) of pNIPAAm. In addition, the diffusive permeability of the hydrogel is switched upon change of temperature, whereby diffusants are trapped above the LCST of pNIPAAm. Moreover, it is possible to disassemble and reform the gel upon change of pH. With that, the hydrogel has potential application as a switchable and reversible membrane.

1. Introduction

Hydrogels are polymer network bodies filled and swollen by water.[1,2] This constitutes "shape-stable water", that is, fluid water held in place by a polymer-network skeleton. The most characteristic and favorable properties of hydrogels are their soft mechanics and high diffusive permeability for molecular diffusants.[3,4] The latter is made possible by slip-through of small molecular-scale diffusants through the nanometer-scale network meshes.[5,6] This property can be used in applications like separation techniques or membrane systems.[7] However, to increase the application spectrum, it is necessary to be able to control the diffusive permeability on demand via an external stimulus; gaining such control is a developing research direction.[8]

A way to achieve such control of the diffusive permeability is to use thermoresponsive membranes, where a thermoresponsive polymer is either attached to a solid substrate or is present in form of a thin hydrogel film.[8–10] In general, diffusion through a polymer-network gel is determined by the mesh size, and this can be controlled in several ways, such as increasing the concentration of the polymer or by changing the structure of the polymer network, for example, through introduction of dangling chains.[11,12] Here, we employ thermoresponsive dangling chains to exquisitely control the mesh size on demand upon switch of temperature. On top of that, in polymer science, as well as in every other branch of materials science, there is an increasing demand for a sustainable footprint, here meaning a gel that is reversible.[13] An advance in the field of thermoresponsive membranes would be to have a switchable material that can not only reversibly change its diffusive permeability upon application of an external trigger like a change of temperature, but that can also improve its mechanical properties upon the application of such a stimulus. To our knowledge, these three properties, namely reversibility, switchable diffusive permeability, and enhanced mechanical properties, have not been yet investigated in the same hydrogel. In this paper, we present a dual dynamic network (DDN) that provides all the above-mentioned needs in one material with the opportunity to tune them in an independent fashion, as it can be visualized in **Figure 1**. For this purpose, we make use of two suitable chemical motifs: for the thermosensitive switchability, we use the most widespread and famous thermoswitchable polymer, which is poly(*N*-isopropylacrylamide) (pNIPAAm).[14] For the reversibility, we make use of terpyridine, which is capable of forming metallo-supramolecular bonds with metal ions.[15] The resultant noncovalent bond is stable like covalent bonds at certain conditions,[16] but degradable at others. To realize a well-defined permeable microstructure,[17] we use four-arm polyethylene glycol (pEG) that is capable of forming a model supramolecular network;[18] this will allow us to rationally understand the switching material properties on the basis of a nanostructural picture. We realized a dual network composed of tetra-arm pEG, in which each arm is functionalized with terpyridine, capable of forming metal–ligand complexes, and a thermoresponsive polymer, pNIPAAm. Reversibility is achieved by treating the gel with acid and

P. Nicolella, D. Lauxen, M. Ahmadi, S. Seiffert
Department of Chemistry
Johannes Gutenberg-Universität Mainz
Duesbergweg 10-14, Mainz D- 55128, Germany
E-mail: sebastian.seiffert@uni-mainz.de

The ORCID identification number(s) for the author(s) of this article can be found under https://doi.org/10.1002/macp.202100076

© 2021 The Authors. Macromolecular Chemistry and Physics published by Wiley-VCH GmbH. This is an open access article under the terms of the Creative Commons Attribution License, which permits use, distribution and reproduction in any medium, provided the original work is properly cited.

DOI: 10.1002/macp.202100076

15213935, 2021, 16, Downloaded from https://onlinelibrary.wiley.com/doi/10.1002/macp.202100076 by Cochrane Germany, Wiley Online Library on [17/10/2022]. See the Terms and Conditions (https://onlinelibrary.wiley.com/terms-and-conditions) on Wiley Online Library for rules of use; OA articles are governed by the applicable Creative Commons License

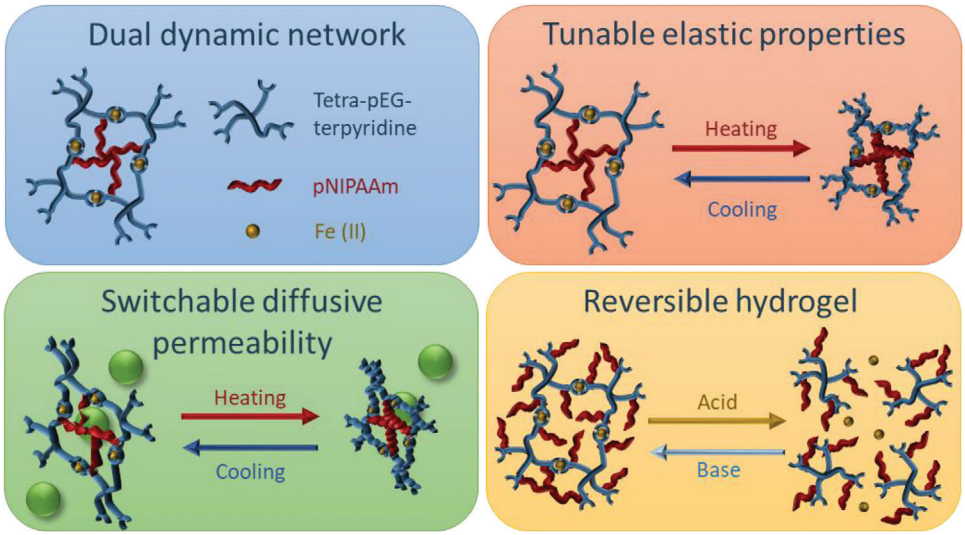

Figure 1. Concept of this work. A dually dynamic polymer network makes it possible to combine multiple properties in one material. Specifically, the diffusive permeability and the elastic modulus of the hydrogel can be tuned with temperature, and the reversibility of the gel can be triggered with pH.

base. The switchable diffusive permeability of the network is investigated via tracer diffusivity probed by fluorescence recovery after photobleaching (FRAP) below and above the lower critical solution temperature (LCST) of pNIPAAm. Macroscopically, the elasticity of the network is investigated with linear rheology upon variation of temperature.

2. Results and Discussion

2.1. Synthesis of the Dual Dynamic Network

The synthesis of the dual dynamic network is sketched in **Scheme 1**. The starting point of the synthesis is a four-arm pEG with terminal –OH groups. These are converted into epoxy rings through the addition of epichlorohydrin. Afterward, the epoxy ring is opened and the pEG then has two functional groups on each arm: one hydroxyl and one azide group. The azide group reacts with propargyl-terpyridine, where the terpyridine (together with the metal) provides the first dynamic moiety. The hydroxyl groups are then transformed first into *N*-hydroxysuccinimidyl (NHS) groups, and afterward these react with amine-functionalized pNIPAAm, to form the second dynamic moiety.

2.2. Dual Dynamic Hydrogels

The aim of this work is to provide a polymer hydrogel that combines switchable elasticity and diffusive permeability as well as reversibility in one material, with independent tunability of these properties. We realize this goal in a dual dynamic hydrogel based on tetra-arm pEG, where each arm provides a double dynamic functionalization. The first functional motif is terpyridine, which is able to form a metal–ligand complex with metal ions. In this work, we used Fe(II) tetrafluoroborate hexahydrate for complexation in stoichiometric amount to the terpyridine, i.e., for every pair of terpyridine there is a metal ion. The second dynamic motif is pNIPAAm graft oligomers, which is a thermoresponsive polymer with an LCST around 32 °C in aqueous surrounding.[14] The cloud point of the complete tetra-pEG-PNIPAAm-terpyridine polymer is probed with UV–vis spectroscopy and taken as an indication of the LCST, denoting it to be 32.5 °C, that is, not distant from the LCST of pure pNIPAAm. We assume that the transition is complete beyond that temperature, as the sample transmittance is afterward constantly zero from there on (see Figure S1 in the Supporting Information). We chose a tetra-pEG basis of 10 000 g mol^{-1} and a pNIPAAm of 5500 g mol^{-1}. There are four pNIPAAm chains for each star-pEG, so the total amount of pNIPAAm in weight is 68.75%. The polymer concentration for the gels is 100 g L^{-1}. So, in a 100 g L^{-1} sample, the concentration of pEG is 31.25 g L^{-1}, and the concentration of pNIPAAm is 68.75 g L^{-1}. With that platform, we form gels that can be switched by toggling the pNIPAAm branches from solvated to collapsed states, thereby toggling the gel-network mesh sizes and hence the gel elasticity, and that can be degraded by dissociation of the iron–terpyridine complexes. To assess this, we probe the gel diffusive permeability by monitoring the diffusivity of a fluorescent probe in the gel with FRAP, and we also study the change in the gel elastic modulus upon switch of temperature below and above the LCST of pNIPAAm in water with rheology. We also study the reversibility of the network upon change of pH.

2.3. Reversibility

To obtain a reversible gel, we include a motif that can be broken and rebuilt on demand; we realize this by terpyridine–metal complexes. Depending on the choice of metal ion, the strength of the complex varies. We chose a "strong" ion such Fe(II), that forms a strong complex with terpyridine that is active at 554 nm of the visible spectrum, giving to the complex a peculiar purple color.[19] This complex is stable in air: during observations over a long time scale (months), we did not observe any change in color. Moreover, Fe(II) has a preference to coordinate with nitrogen atoms rather

© 2021 The Authors. Macromolecular Chemistry and Physics published by Wiley-VCH GmbH

15213935, 2021, 16, Downloaded from https://onlinelibrary.wiley.com/doi/10.1002/macp.202100076 by Cochrane Germany, Wiley Online Library on [17/10/2022]. See the Terms and Conditions (https://onlinelibrary.wiley.com/terms-and-conditions) on Wiley Online Library for rules of use; OA articles are governed by the applicable Creative Commons License

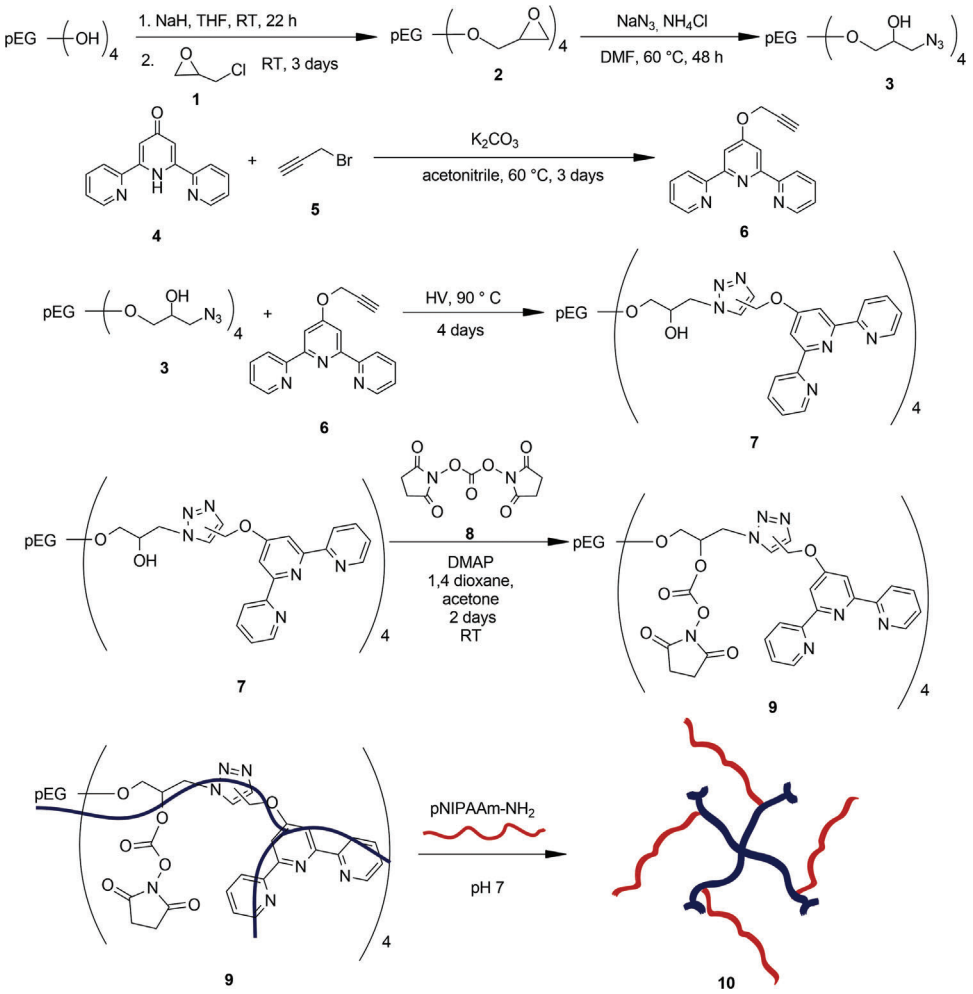

Scheme 1. Synthesis of the dual dynamic network composed of tetra-pEG-pNIPAAm-terpyridine (**10**).

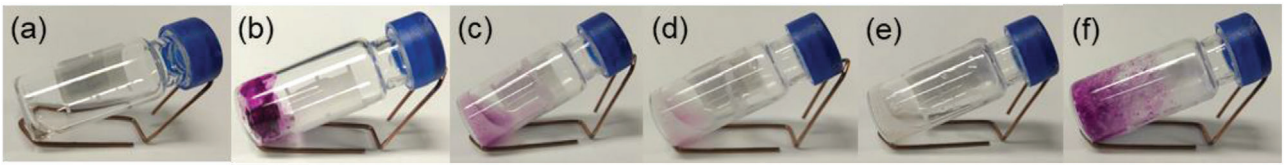

Figure 2. Reversibility of the double dynamic kind of gel treated in this work. The polymer solution (a) is mixed with Fe(II) and forms a gel (b). Upon addition of HCl, the metal complex between the iron and the terpyridine breaks (c–d), and the gel turns into a sol (e). Upon addition of NaOH, the metal complex forms again and the gel is restored (f).

than oxygen atoms, in contrast to its oxidated form Fe(III), that has preference to be in coordination with oxygen atoms.[20] Complexes with iron can be as strong as covalent bonds, but by change of the ion oxidation state, that strength can be drastically altered. For example, hydrogels with Fe(II) are durable and appear like covalent gels, whereas hydrogels with Fe(III) are fluidic on long timescales. If the aim is to weaken the gel, then oxidation of the metal ion is the way to go; however, since we intend to achieve a complete disassembly and not only a weakening of the network, we use a different approach and act on the bond between the terpyridine and the metal ion rather than just on the metal ion. Based on that premise, we form a hydrogel by adding 10 µL of Fe(II) solution to a 90 µL concentrated solution of pEG-pNIPAAm terpyridine, thereby achieving a total polymer concentration of 100 g L^{-1} in the gel. To the 100 µL gel, 30 µL of 37% HCl solution are added, and the flask is vortexed vigorously. Decomplexation is achieved in about 20 min, as shown in **Figure 2**.

As it can be seen in Figure 2b–e, upon addition of the acid, the color of the gel changes from purple to colorless gradually. The gel linking nodes decomplex because the acid protonates the nitrogen atoms of the terpyridine that are therefore no more capable of forming the complex with the iron. This way, the complex between the terpyridine and the iron is broken and the network disassembles. However, this process is reversible. By using a base, such as NaOH, the terpyridine is deprotonated and the nitrogen atoms can form again the supramolecular bond with the

© 2021 The Authors. Macromolecular Chemistry and Physics published by Wiley-VCH GmbH

15213935, 2021, 16, Downloaded from https://onlinelibrary.wiley.com/doi/10.1002/macp.202100076 by Cochrane Germany, Wiley Online Library on [17/10/2022]. See the Terms and Conditions (https://onlinelibrary.wiley.com/terms-and-conditions) on Wiley Online Library for rules of use; OA articles are governed by the applicable Creative Commons License

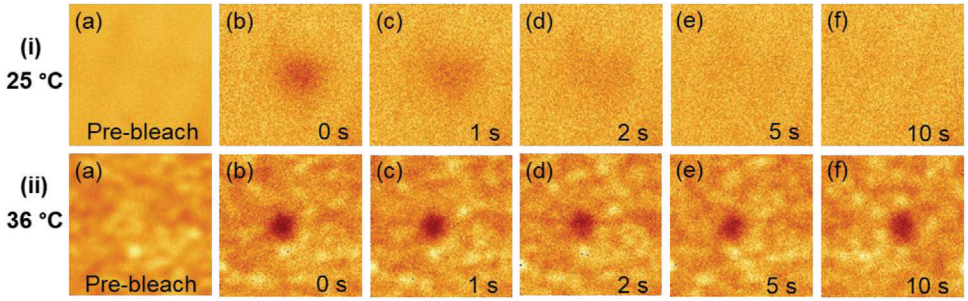

Figure 3. FRAP measurements of the dual dynamic hydrogel performed below i) and above ii) the LCST of pNIPAAm in water, where the diffusive probe is a tetra-pEG functionalized with rhodamine B. The first image of each series (a) is before the bleaching, the second image (b) is at the bleaching, while the others (c–f) are taken respectively after 1, 2, 5, and 10 s. Below the LCST, the bleached spot disappears within the first 5 s, whereas above the LCST, the bleached spot remains. Each image is about 50 × 50 μm^2.

iron. To reform the gel, 20 µL of 50% NaOH solution is added and the solution is vortexed. Upon that, the gel forms back within 10 min and regains its purple color, indicating that the bond between the terpyridine and the iron has reformed again.

2.4. Switchable Diffusive Permeability

The diffusive permeability of the network is assessed by monitoring the diffusivity of a macromolecular probe within the gel with FRAP. To see how the permeability changes upon switch of temperature, FRAP measurements are done below and above the LCST of pNIPAAm in water, respectively at 25 and 36 °C. The fluorescent probe is a four-arm pEG 10 000 g mol^{-1} functionalized with rhodamine B. FRAP measurements are performed in a custom-made cell that allows the temperature to be controlled with ±1 °C precision. In FRAP, a fluorescent probe that is incorporated in the sample is bleached with high intensity laser light in a spot in the sample. In that spot, the bleaching produces a dark region with Gaussian radial intensity profile of the extent of bleaching, exhibiting typical width (measured as the variance of the Gaussian) of about 2 µm right after bleaching. After the bleaching, a series of post-bleach images are recorded at fixed time intervals. During that period, bleached molecules diffuse outside the spot whereas not-bleached molecules diffuse inside of it. This exchange of bleached and unbleached molecules leads to diffusive smearing of the Gaussian, which can be quantified and analyzed by comparison to analytical functions that solve the diffusion equation for that kind of initial and boundary conditions. As a result, we obtain the translational diffusion coefficient.[21] If the data fitting is done with a superposition of multiple Gaussians, we obtain a distribution of diffusion coefficients, thereby appropriately treating polydisperse diffusion scenarios.[22] In our work, we compare how the diffusion of tetra-pEG-rhodamine is influenced by the temperature in the tetra-pEG-pNIPAAm-terpyridine hydrogel respectively below and above the LCST of pNIPAAm in water.

In **Figure 3**, the FRAP series of images are shown for 25 °C i) and 36 °C ii). The first images (a) display the prebleach situation and are the result of an averaging of four pictures. Image (b) shows the sample immediately after the bleaching. Images (c–f) represent the evolution upon diffusion respectively after 1, 2, 5, and 10 s after the bleach. As it can be seen in Figure 3i, in the case of the sample at 25 °C, the bleached spot disappears within the first 5 s, whereas, as it can be seen from Figure 3ii, in the case of 36 °C, the bleached spot remains constant in the considered timeframe.

Diffusion coefficients are calculated by averaging six measurements for each temperature and calculating the standard error. The Gaussian curves relative to the two temperatures can be found in Figure S2 (Supporting Information) where it can be noticed that the number of curves at room temperature is low compared to the ones at higher temperature, due to the fact that the bleaching spot disappears fast at room temperature. At 25 °C, the average diffusion coefficient is (9.46 ± 1.53) $\mu m^2\ s^{-1}$, while at 36 °C, the average diffusion coefficient is (0.10 ± 0.07) $\mu m^2\ s^{-1}$. Hence, above the LCST of pNIPAAm, the diffusion coefficient is almost two orders of magnitude smaller than at room temperature. This means that the diffusion of the fluorescent probe is drastically hindered above the LCST of pNIPAAm. This can be ascribed to the pNIPAAm chains that collapse and aggregate with each other in the gel network at those conditions, thereby blocking the passage of the dye-labeled probe by forming an obstacle for the diffusion of the probe between the meshes. To further investigate the system, the same FRAP experiments were performed by probing the diffusion of only the dye. For this purpose, the tetra-pEG-pNIPAAm-terpyridine was mixed with a solution of rhodamine B isocyanate having the same concentration of the dye on the pEG-rhodamine probe. By performing the experiment above the LCST, it could be noted that also in the case of only dye, the bleaching spot stayed. Therefore, the decrease in the diffusion coefficient of the fluorescent dyes results from the combination of two effects. On one side there is the decrease of the mesh sizes due to the aggregation of multiple collapsing pNIPAAm chains, as manifesting itself also in rheology, and on the other side there is the contribution of the interaction and partial entrapment of the dye molecules with pNIPAAm. Moreover, it is observed that the total volume of the hydrogel remains constant with temperature (see Figures S3 and S4 in the Supporting Information). Therefore, the volume shrinks locally due to the collapsing of the pNIPAAm chains, and there will then be highly concentrated zones where the diffusion of the probe is completely blocked and less concentrated zones where the probe can still diffuse. Therefore, there is still some diminished but not completely vanished mobility of the traces. This interpretation is supported visually in Figure 3, where the sample above the LCST

© 2021 The Authors. Macromolecular Chemistry and Physics published by Wiley-VCH GmbH

15213935, 2021, 16, Downloaded from https://onlinelibrary.wiley.com/doi/10.1002/macp.202100076 by Cochrane Germany, Wiley Online Library on [17/10/2022]. See the Terms and Conditions (https://onlinelibrary.wiley.com/terms-and-conditions) on Wiley Online Library for rules of use; OA articles are governed by the applicable Creative Commons License

shows brighter and darker spots. Prospectively, super-resolution microscopy techniques could be employed to characterize that type of sample heterogeneity. These heterogeneities derive from the microphase-separation and the aggregation of pNIPAAm in bigger clusters. Below LCST, by contrast, the probe species can diffuse quite freely within the gel. This pronounced difference in molecular mobility provides a useful means for the development of thermoresponsive membranes with switchable diffusive permeability.

2.5. Tunable Elastic Properties

To test the change of the elastic properties of the gel, rheological measurements are performed. For this purpose, frequency sweeps are recorded at 25 and 35 °C, respectively below and above the LCST of the pNIPAAm chains in the samples. In addition, temperature cycles are performed to study the elastic response on a larger scale of temperatures.

2.5.1. Frequency Sweeps

To test the temperature dependence of the elastic modulus of the polymer below and above the LCST of the pNIPAAm chains in the samples, frequency sweeps are recorded from 20 to 0.01 rad s^{-1}, respectively at 25 and at 35 °C with a shear amplitude of γ = 1%. To avoid rupture of the gel with the transfer to the rheometer, the gel is formed directly on the instrument with a polymer concentration of 100 g L^{-1}.

The storage (full symbols) and loss (empty symbols) moduli are shown as a function of the frequency at 25 °C (blue) and 35 °C (red), respectively, below and above the LCST of pNIPAAm, as shown in **Figure 4**. The rheological spectra display that G' and G'' are constant in the considered frequency range. This covalent-gel like signature is caused by the strong complexes that iron forms with the terpyridine. Upon increase of the temperature from 25 to 35 °C, the elastic modulus doubles from 1000 Pa to 2000 Pa. Qualitatively, this finding is explainable by the microphase-separation of the pNIPAAm chains above their LCST in our hydrogels, which creates domains that act as additional crosslinks, thereby enforcing the gel. Quantitatively, though, these values are still lower than their estimates calculated with the phantom-network model, that are 7740 and 8002 Pa, respectively, for 25 and 35 °C. There are several factors that can contribute to lowering the modulus, and the main factor is probably network defects and inhomogeneities.[23] The theoretical value of the modulus is calculated taking into account a perfectly homogeneous network where each arm is an elastically active chain. However, in real networks there are defects and inhomogeneities such as dangling chains, loops, and spatial variation of the crosslinking density.[23] These could be also partially due to the steric hindrance of the pNIPAAm chains in proximity of the terpyridine group. From the elastic modulus, we can also estimate the average mesh size of the hydrogel network as $\xi = (RT/G'N_A)^{1/3}$, where R is the gas constant (8.13 J mol^{-1} K^{-1}), T is the temperature (respectively 298.15 K and 308.15 K), G' is the elastic modulus and N_A is the Avogadro constant.[24] With that simple estimate, the average mesh size at 25 °C is found to be 16 nm, whereas the one at 35 °C

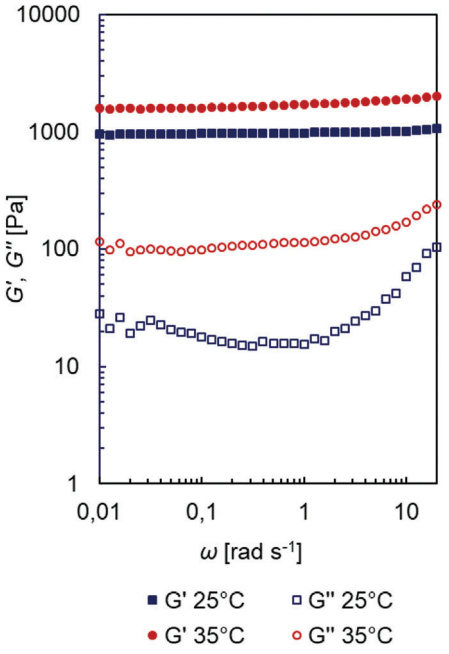

Figure 4. Frequency dependence of the storage modulus (full symbols) and loss modulus (empty symbols) at 25 °C (blue squares) and 35 °C (red circles) of the dual dynamic hydrogel, for a polymer concentration of 100 g L^{-1} and measured with a shear amplitude of γ = 1%.

is 13 nm. This mesh size is reasonable, as the average distance between pNIPAAm dangling chains calculated through its molar concentration is 8 nm.[25]

2.5.2. Temperature Cycles

To further study the temperature-dependence of the storage and loss moduli in an even extended temperature range, temperature cycles are recorded between 10 and 40 °C with γ = 1% and ω = 1 rad s^{-1} for a polymer concentration of 100 g L^{-1}. First, the sample is allowed to equilibrate at 10 °C, and then a heating ramp is performed up to 40 °C. After equilibrating the sample at 40 °C, a cooling ramp is performed back down to 10 °C with the same rate as the heating ramp. A complete heating–cooling cycle is shown in **Figure 5**.

The storage and loss moduli are linear from 10 to 32 °C. From 32 °C, the pNIPAAm starts to phase-separate. This can be seen in the heating cycle with an increase of both the storage and loss moduli. While the elastic modulus increases smoothly, the loss modulus increases more steeply, with an inflection point around the LCST of pNIPAAm. At 40 °C, the elastic modulus has doubled and the loss modulus has increased of one order of magnitude, compared to their respective values at 10 °C. The cooling cycle shows hysteresis around the LCST for both moduli. This can be explained by considering that when the pNIPAAm chains collapse due to phase separation, they form clusters, and the time and/or energy needed for breakage of these clusters causes a hysteresis in our kind of experimental assessment. From 30 °C, the cooling cycle overlaps with the heating cycle again. This means that the material recovers completely and that its elastic properties are reversible.

© 2021 The Authors. Macromolecular Chemistry and Physics published by Wiley-VCH GmbH

15213935, 2021, 16, Downloaded from https://onlinelibrary.wiley.com/doi/10.1002/macp.202100076 by Cochrane Germany, Wiley Online Library on [17/10/2022]. See the Terms and Conditions (https://onlinelibrary.wiley.com/terms-and-conditions) on Wiley Online Library for rules of use; OA articles are governed by the applicable Creative Commons License

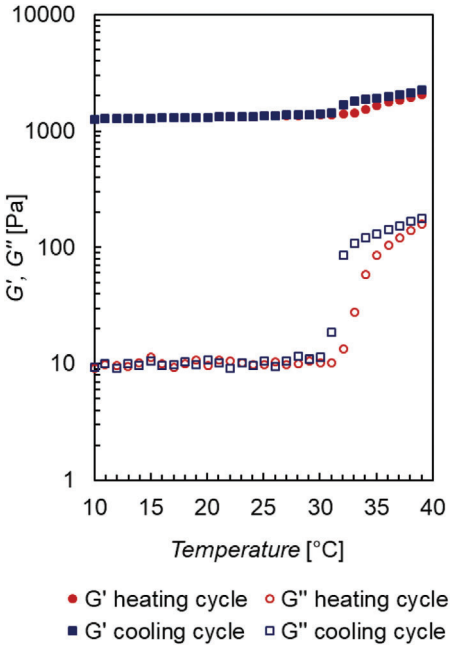

Figure 5. Temperature dependence of the storage modulus (full symbols) and loss modulus (empty symbols) recorded at $\gamma = 1\%$ and $\omega = 1$ rad s^{-1} for a polymer concentration of 100 g L^{-1}. The red dataset (circles) denotes the heating cycle and the blue dataset (squares) denotes the cooling cycle. Around the LCST, a hysteresis in the cooling cycle is observed.

3. Conclusion

The multifunctional dual dynamic polymer network introduced in this work proved a material platform that has switchable diffusive permeability and is reversible with the possibility to tune these properties independently from each other. Reversibility can be achieved by acidification, whereby the gel can be recovered with a base. In addition, switchable diffusive permeability can be achieved by varying the temperature. Along with that, the gel doubles its elastic modulus upon heating. Combining all these properties in one material is appealing for separation or membrane applications. Further studies may include different lengths of the thermoresponsive graft polymer and use of different metal ions for the metallo-supramolecular junctions, thereby exploring the range of switchability and reversibility.

4. Experimental Section

Synthesis–Materials: Tetra-hydroxyl polyethylene glycol (pEG) (10 000 g mol^{-1}) was purchased from JenKem Technology (Plano, Texas, USA). Tetra-pEG-amine (10 000 g mol^{-1}) was purchased from Biochempeg Scientific. Amine-functionalized pNIPAAm (5500 g mol^{-1}) was purchased from Sigma Aldrich. Sodium hydride 57–63 wt% oil dispersion and 4-(dimethylamino)-pyridine 99% were purchased from Alfa Aesar (Thermo Fisher). Tetrahydrofuran 99.8% (THF), dichloromethane 99.8% (DCM), diethyl ether 99.5%, dimethylformamide 99.5% (DMF), methanol 99.8%, sodium chloride, and potassium carbonate (anhydrous) were purchased from Fisher Scientific. Sodium azide 99% and sodium carbonate (anhydrous) 99.5% were purchased from Fluka. Epichlorohydrin 99%, magnesium sulphate 97% (pure anhydrous), ammonium chloride, dry 1,4 dioxane 99.5%, acetonitrile 99.99%, and propargyl bromide 80 wt% in toluene were purchased from Acros Organics. Potassium dihydrogen phosphate 99% was purchased from ROTH. Activated carbon Norit A was purchased from Aldrich Chemical Company Inc. 2,6-bis (2-Pyridyl)-4(1H)-pyridone 98% was purchased from TCI. Chloroform Uvasol and sodium hydroxide solution 50% were purchased from Merck. Hydrochloric acid 37%, *n*-heptane, and di-sodium hydrogen phosphate anhydrous were purchased from VWR Chemicals. Dimethylsulfoxide-d_6 99.8% (DMSO) was purchased from Deutero. Iron(II) tetrafluoroborate hexahydrate 97%, rhodamine B isocyanate, and *N,N′*-disuccinimidyl carbonate 95%, were purchased from Aldrich.

Tetra-pEG-Epoxide (***2***): Tetra-pEG-hydroxyl 10 000 g mol^{-1} (13.06 g, 1.306 mmol, 1 eq.) is melted at 80 °C in high vacuum. The temperature is decreased to 40 °C and dry THF (320 mL) is added for dissolution. Sodium hydride 60 wt% in mineral oil (1.67 g, 41.79 mmol, 32 eq.) is added at room temperature and the mixture is stirred for 22 h. Afterward, epichlorohydrin (**1**) (8.2 mL, 104.48 mmol, 80 eq.) is added and the solution is stirred for 3 days. Few drops of distilled water are added and the product is extracted five times with DCM (300 mL) and brine (50 mL). Afterward, it is dried with magnesium sulphate and filtered. The concentrated solution is precipitated in cold diethyl ether (1 L), stirred for 30 min, filtered, and dried overnight in high vacuum (yield 80.5%). ^{1}H-NMR (DMSO-d_6, 400 MHz, δ = ppm): 3.70 (m, 3H), 3.51 (m, 909H, pEG backbone), 3.25 (m, 3H), 3.09 (m, 3H), 2.72 (m, 3H), 2.52 (s, 1H), 3.87 (s, 4H).

Tetra-pEG-Hydroxy-Azide (***3***): Tetra-pEG-epoxide (**2**) (10.63 g, 1.04 mmol, 1 eq.) is dissolved in DMF (110 mL), then sodium azide (2.77 g, 42.65 mmol, 41 eq.) and ammonium chloride (4.54 g, 84.88 mmol, 82 eq.) are added and the solution is stirred for 48 h at 60 °C. The product is extracted three times with brine (50 mL) and DCM (400 mL). Afterward, it is dried with magnesium sulphate, filtered, distilled, and precipitated in cold diethyl ether (1 L). After stirring for 30 min, it is filtered and dried overnight in high vacuum (yield 67%). ^{1}H-NMR (DMSO-d_6, 400 MHz, δ = ppm): 5.25 (d, 3H), 3.77 (m, 3H), 3.68 (m, 5H), 3.51 (m, 909H, pEG backbone), 3.37 (m, 5H), 3.25 (d, 10H), 3.19 (m, 3H).

Propargyl-Terpyridine (***6***): To obtain the propargyl-terpyridine (**6**), potassium carbonate (10.08 g, 72.938 mmol, 6.1 eq.) is dried in high vacuum for 90 min, and then 2,6-bis(2-pyridyl)-4(1H)-pyridone (**4**) (3 g, 12.035 mmol, 1 eq.) is added. The reagents are suspended in dry acetonitrile (120 mL) for 2 h, and afterward propargyl bromide (**5**) (9.2 M in toluene, 1.6 mL, 14.72 mmol, 1.2 eq.) is added dropwise. The mixture is stirred for 3 days at 60 °C and then precipitated in cold water (500 mL), filtered and dried overnight in high vacuum. In order to have a colorless product, the resulting propargyl-terpyridine is dissolved in *n*-heptane (500 mL) at 98 °C and two spoons of active carbon are added. Then, the suspension is filtered over a hot funnel with an ice bath around the flask for recrystallization. Afterward, the product is filtered and dried overnight in high vacuum (yield 52%). ^{1}H-NMR (DMSO-d_6, 400 MHz, δ = ppm): 8.74 (ddd, 2H), 8.62 (dt, 2H), 8.05 (s, 2H), 8.01 (td, 2H), 7.51 (ddd, 2H), 5.11 (d, 2H), 3.72 (t, 1H).

Tetra-pEG-Hydroxy-Terpyridine (***7***): Tetra-pEG-hydroxy-azide (**3**) (7.15 g, 0.688 mmol, 1 eq.) is dried in high vacuum for 30 min. Afterward, propargyl-terpyridine (**6**) (1.64 g, 5.708 mmol, 8.3 eq.) is added, and the mixture is heated to 90 °C. It is stirred under high vacuum at 90 °C for 4 days. After cooling the temperature down to 40 °C, DCM (50 mL) is added. The solution is precipitated in cold diethyl ether (1 L) and stirred for 30 min. Afterward, it is filtered and dried overnight in high vacuum (yield 78%). The degree of functionalization is assessed by UV–vis spectroscopy in chloroform Uvasol to be 90% and with H-NMR to be 75–87.5%. This difference in functionality might be due to phase/baseline correction in the NMR spectra. However, this 10% difference should not impact the properties of the hydrogel, as a lower functionalization falls together with the effect of defects, such as for example dangling chains, as discussed before. Moreover, in case there would be an additional effect, it would be the same for both temperatures and therefore the relative behavior that is investigated would not change. ^{1}H-NMR (DMSO-d_6, 400 MHz, δ = ppm): 8.73 (m, 6H), 8.63 (m, 6H), 8.21 (s, 1H), 8.10 (d, 6H), 8.02 (m, 6H), 7.88 (s, 1H), 7.51 (m, 6H), 5.61 (s, 2H), 5.45 (s, 4H), 5.37 (d, 1H), 5.32 (d, 2H), 4.45 (m, 7H), 4.00 (m, 4H), 3.68 (t, 5H), 3.47 (m, 909H, pEG backbone), 1.24 (s, 1H).

© 2021 The Authors. Macromolecular Chemistry and Physics published by Wiley-VCH GmbH

15213935, 2021, 16, Downloaded from https://onlinelibrary.wiley.com/doi/10.1002/macp.202100076 by Cochrane Germany, Wiley Online Library on [17/10/2022]. See the Terms and Conditions (https://onlinelibrary.wiley.com/terms-and-conditions) on Wiley Online Library for rules of use; OA articles are governed by the applicable Creative Commons License

*Tetra-pEG-N-Hydroxysuccinimide-Terpyridine (**9**)*: Tetra-pEG-hydroxy-terpyridine (**7**) (6.2 g, 0.537 mmol, 1 eq.) is dried for one hour in high vacuum. Afterward, dry 1,4-dioxane (30 mL) is added, and the tetra-pEG-hydroxy-terpyridine is dissolved at 40 °C. At the same time, *N,N′*-disuccinimidyl carbonate (**8**) (1.10 g, 4.298 mmol, 8 eq.) is dissolved in dry acetone (10 mL) and 4-dimethylaminopyridine (DMAP) (0.53 g, 4.338 mmol, 8.1 eq.) is dissolved in dry acetone (10 mL). To the *N,N′*-disuccinimidyl carbonate suspension, first the tetra-pEG-hydroxy-terpyridine and then the DMAP are added dropwise. The solution is stirred for 2 days and then precipitated in cold diethyl ether (500 mL). After filtering, the product is dried overnight in high vacuum (yield 78%). ^{1}H-NMR (DMSO-d_6, 400 MHz, δ = ppm): 8.73 (d, 6H), 8.63 (m, 6H), 8.28 (s, 2H), 8.10 (m,6H), 8.02 (m, 6H), 7.52 (m, 6H), 5.47 (m, 10H), 4.77 (m, 7H), 3.47 (m, 909H, pEG backbone), 2.78 (m, 13H).

*Tetra-pEG-pNIPAAm-Terpyridine (**10**)*: Amine-functionalized pNIPAAm is attached to the tetra-pEG-*N*-hydroxysuccinimide-terpyridine **(9)** via a click reaction. For this purpose, a buffer solution (500 mL) with a pH value of 7 is prepared with potassium dihydrogen phosphate (3.52 g, 25.871 mmol) and disodium hydrogen phosphate (5.79 g, 40.798 mmol). A neutral pH is achieved with addition of 50% sodium hydroxide solution. Tetra-pEG-*N*-hydroxysuccinimide-terpyridine (**9**) (1.01 g, 0.083 mmol, 1.0 eq.) and 5500 g mol^{-1} amine-terminated pNIPAAm (3.93 g, 0.714 mmol, 8.6 eq.) are dissolved in the buffer solution (100 mL) and stirred overnight. Afterward, the solution is freeze dried, and the unreacted pNIPAAm is separated by dialysis over two weeks, with membranes having a MWCO value of 6–8 kDa (yield 106%). The success of the chain-end functionalization is determined with DOSY-NMR (see Figures S14–S16 in the Supporting Information), as in the spectra of the copolymer, the pEG and the pNIPAAm show the same diffusion coefficient being 20.9 μm^2 s^{-1} for the pNIPAAm and 19.6 μm^2 s^{-1} for the pEG, thereby denoting them to be one united species, whereas the free pNIPAAm shows a faster diffusion coefficient of 30.1 μm^2 s^{-1}.

The degree of functionalization can be determined with NMR by comparison of the integrated peaks of the pEG backbone and of the pNIPAAm. The integrals of the pNIPAAm chains show an additional 30% in respect to the theoretical values, and the total reaction yield is 106%. Even though the pNIPAAm content has halved during dialysis, as it can be observed by comparing the integrated pNIPAAm peaks in the NMR spectra before and after dialysis (see Figures S12 and S13 in the Supporting Information), there is an additional percentage of loose pNIPAAm chains that are still in the network and that were not possible to dialyze out. These pNIPAAm chains will certainly collapse above the LCST, and in case they are in proximity of the graft chains in the network, they might take part in the clusters. However, it is not expected that these loose chains have a marked influence on the network properties as they are not connected to the network. The cloud point of the tetra-pEG-pNIPAAm-terpyridine, is assessed via UV–vis spectroscopy to be 32.5 °C by measuring the transmittance at different temperatures and extrapolating the inflection point of the curve and taking it as an indication of the LCST. ^{1}H-NMR before dialysis (DMSO-d_6, 400 MHz, δ = ppm): 8.72 (m, 7H), 8.62 (m, 8H), 8.21 (s, 2H), 8.04 (m, 17H), 7.54 (m, 17H), 7.18 (m, 479H), 6.15 (m, 6H), 5.67–5.49 (m, 11H), 4.62 (s, 6H), 3.84 (s, 556H, pNIPAAm), 3.50 (s, 909H, pEG), 1.96 (s, 522H, pNIPAAm), 1.45 (m, 1225H, pNIPAAm), 1.04 (s, 2697H, pNIPAAm).

^{1}H-NMR after dialysis (DMSO-d6, 400 MHz, δ = ppm): 8.73 (m, 7H), 8.63 (m, 6H), 8.22 (d, 2H), 8.10 (m,7H), 8.01 (m, 6H), 7.52 (m, 6H), 7.16 (m, 252H pNIPAAm), 5.61 (s, 3H), 5.45 (s, 4H), 5.08 (m, 2H), 4.67 (m, 1H), 3.85 (m, 286H, pNIPAAm), 3.49 (m, 909H, pEG backbone), 1.98 (s, 335H, pNIPAAm), 1.46 (m, 623H, pNIPAAm), 1.12 (m, 1898H, pNIPAAm).

All NMR spectra can be found in the Supplementary Information.

Tetra-pEG-Rhodamine B: For FRAP experiments, a fluorescent probe is synthesized, composed of four-arm 10 000 g mol^{-1} pEG, functionalized with rhodamine B. For this purpose, a saturated solution (200 mL) of sodium carbonate in methanol is prepared, and tetra-pEG-amine 10 000 g mol^{-1} (0.51 g, 0.051 mmol, 1 eq.) is added to it. In a flask covered with aluminum foil, rhodamine B isothiocyanate (0.333 g, 0.621 mmol, 12 eq.) is dissolved in dry methanol (40 mL). After dissolution, it is added to the sodium carbonate solution dropwise. The mixture is stirred under argon for 4 days in the dark. Then, ammonium chloride (0.722 g, 13.498 mmol, 265 eq.) and methanol (30 mL) are added and the mixture is stirred overnight. The product is precipitated twice in ice-cold diethyl ether (1 L), filtrated, and dried overnight in high vacuum. Afterward, it is dissolved in methanol (30 mL) and passed through a Sephadex LH-20 column. The fractions of the product are collected and the solvent is removed via rotary evaporation. Then, the product is dissolved in DCM (5 mL), precipitated in diethyl ether (600 mL), and dried overnight in high vacuum (yield 36%). The degree of functionalization is determined with UV–vis spectroscopy to be 34%. Despite the 12 equivalents of rhodamine, it was not possible to achieve a 100% functionalization, since the intended degree of functionalization was already high. The degree of labeling, which is 2% of the monomer units, is already higher than the usual degree of functionalization used. A 34% functionalization means that every star carries on average at least one fluorophore and this is sufficient for FRAP characterization. ^{1}H-NMR (DMSO-d_6, 400 MHz, δ = ppm): 8.72 (m, 8H), 3.51 (m, pEG backbone, 909 H), 1.09 (m, 12H), 6.56 (m, 4H), 7.05 (m, 5H).

Methods–Reversibility: Gels are prepared in milli-Q water with 100 g L^{-1} concentration of polymer and a stoichiometric amount of Fe(II) tetrafluoroborate hexahydrate in respect to the terpyridine (one metal ion for two terpyridines). To a 90 μL polymer solution, 10 μL of metal solution is added and immediately vortexed. The complexation between the terpyridine and the iron gives the gel a characteristic purple color.[19] To a 100 μL of 100 g L^{-1} gel, 30 μL of 37% solution of HCl is added and everything is vortexed. Decomplexation occurs within 20 min with repeated vortexing. During decomplexation the gel loses the characteristic purple color of the iron–terpyridine complex and becomes colorless again. The original gel is recovered by adding 20 μL of a 50% solution of NaOH, whereupon the gel recovers in about 10 min.

FRAP: FRAP measurements are performed on a Leica TCS SP2 microscope with 10x dry objective of NA 0.3 at 30× zoom. The excitation wavelength is 543 nm (He-Ne Laser) at 18–19% of its full intensity for 25 °C and at 12–18% for 36 °C. Bleaching is achieved with 100% intensity of the 458 nm (Ar Laser), 488 nm (Ar Laser), 514 nm (Ar Laser), and 543 nm (He-Ne Laser) lines. The detection wavelength is 550–600 nm. The image resolution is 128 × 128 pixels, resulting in 50.7 × 50.7 μm^2 recorded images at the utilized zoom level. Scans are performed bidirectional with a line scanning speed of 400 Hz. Before bleaching, four images are recorded and averaged. The bleaching time is set to 1 s, and after the bleaching, a series of images is recorded with a time between the images of 354 ms. For all that, the sample is placed in a custom-made measuring cell that is connected to a power supply for temperature control. Measurements below the LCST of pNIPAAm are performed at about 25 °C, whereas measurements above the LCST are performed at around 36 °C. Below the LCST, 50 pictures are recorded, while above the LCST 300 pictures are recorded after the bleaching. Analysis of the data is done with a multicomponent diffusion model.[22] As fluorescent diffusive probe, four-arm pEG of the same molar mass as the tetra-pEG in the network (10 000 g mol^{-1}) is functionalized with rhodamine B. To 10 mg of tetra-pEG-pNIPAAm-terpyridine, 1.1 mg of the fluorescent probe is added and they are dissolved together in 90 μL of milli-Q water. Then, 10 μL of a solution of Fe(II) tetrafluoroborate hexahydrate in stoichiometric ratio to the terpyridine is added. The gel is prepared the day before, allowed to equilibrate overnight, and then transferred into the measuring chamber.

Rheology: Rheological studies are performed on a stress-controlled Anton Paar Physica MCR 302 rheometer equipped with a parallel plate geometry with 8 mm diameter. To account for the thermal expansion of the geometry with temperature, the geometry is positioned on the bottom plate of the rheometer at 25 °C for 20 min. Experiments are performed with a polymer concentration of 100 g L^{-1}, and the gel is formed directly on the rheometer. 70 μL of tetra-pEG-pNIPAAm-terpyridine solution is poured with a pipette on the bottom plate of the rheometer. The upper geometry is lowered, so that the upper plate would come in contact with the polymer solution, and then lifted up again. 7.77 μL of Fe(II) tetrafluoroborate hexahydrate solution with stoichiometric amount of metal ions to terpyridine is pipetted to the center of the polymer solution. Since the gelation starts instantaneously, the upper geometry is immediately lowered again. To ensure better mixing, and consequently gelation, of

© 2021 The Authors. Macromolecular Chemistry and Physics published by Wiley-VCH GmbH

15213935, 2021, 16, Downloaded from https://onlinelibrary.wiley.com/doi/10.1002/macp.202100076 by Cochrane Germany, Wiley Online Library on [17/10/2022]. See the Terms and Conditions (https://onlinelibrary.wiley.com/terms-and-conditions) on Wiley Online Library for rules of use; OA articles are governed by the applicable Creative Commons License

the polymer solution and the metal ions, the upper geometry is lifted up and lowered again a couple of times. Afterward, a dynamic time sweep is performed at 25 °C with a constant frequency of 1 rad s^{-1} and shear amplitude of 1%, until the sample is fully equilibrated, manifesting itself such that the storage and loss modulus are constant with time. Amplitude sweeps are performed at each temperature to ensure measurements in the linear regime. At 25 °C, with a frequency of 20 rad s^{-1}, the sample shows linear regime in the range of $\gamma = 0.1$–40%. A frequency sweep from 20 to 0.01 rad s^{-1} is performed with an amplitude of $\gamma = 1\%$. Afterward, the sample is heated to 35 °C and allowed to equilibrate again at this temperature with a dynamic time sweep with constant frequency of 1 rad s^{-1} and shear of 1%. Afterward, an amplitude sweep is carried out at 35 °C. With a frequency of 20 rad s^{-1}, the sample shows a linear regime in the range $\gamma = 0.1$–10%. Next, a frequency sweep at 35 °C is performed from 20 rad s^{-1} to 0.01 rad s^{-1} with $\gamma = 1\%$. Then, the sample is brought to 10 °C and let equilibrate again with a dynamic time sweep. A temperature sweep is performed by increasing the temperature of 1 °C every 45 s, from 10 to 40 °C, with frequency of 1 rad s^{-1} and shear of 1%. After equilibrating the sample at 40 °C, it is cooled down at the same rate of the heating cycle, from 40 °C to 10 °C, with frequency of 1 rad s^{-1} and shear of 1%.

Supporting Information

Supporting Information is available from the Wiley Online Library or from the author.

Acknowledgements

This work was financially supported by funding from the H2020 Programme (MARIE SKŁODOWSKA-CURIE ACTIONS) of the European Commission's Innovative Training Networks (H2020-MSCA-ITN-2017) under DoDyNet REA Grant Agreement No. 765811. The authors thank Holger Adams for the construction of the FRAP measurement cell. Paola Nicolella thanks Marco Cirelli, Christina Pyromali, and Katharina Breul for useful discussions.

Open access funding enabled and organized by Projekt DEAL.

Conflict of Interest

The authors declare no conflict of interest.

Data Availability Statement

The data that support the findings of this study are available from the corresponding author upon reasonable request.

Keywords

dual dynamic networks, FRAP, hydrogels, metal–complex hydrogels, pNIPAAm

Received: February 28, 2021
Revised: July 1, 2021
Published online: July 16, 2021

[1] S. Seiffert, *Polym. Chem.* **2017**, *8*, 4472.
[2] F. Di Lorenzo, S. Seiffert, *Polym. Chem.* **2015**, *6*, 5515.
[3] J. P. Gong, *Soft Matter* **2010**, *6*, 2583.
[4] T. Rossow, A. Habicht, S. Seiffert, *Macromolecules* **2014**, *47*, 6473.
[5] A. S. Hoffman, *Adv. Drug Delivery Rev.* **2012**, *64*, 18.
[6] T. Fujiyabu, X. Li, U. - Chung, T. Sakai, *Macromolecules* **2019**, *52*, 1923.
[7] M. K. Yazdi, V. Vatanpour, A. Taghizadeh, M. Taghizadeh, M. R. Ganjali, M. T. Munir, S. Habibzadeh, M. R. Saeb, M. Ghaedi, *Mater. Sci. Eng., C* **2020**, *114*, 111023.
[8] R. Ghosh, in *Functional Biopolymers* (Eds: M. A. J. Mazumder H. Sheardown, A. Al-Ahmed), Springer Nature, Switzerland, **2019**, Ch. 15.
[9] L. Chu, R. Xie, X. Ju, *Chin. J. Chem. Eng.* **2011**, *19*, 891.
[10] I. Tokarev, S. Minko, *Adv. Mater.* **2010**, *22*, 3446.
[11] J. Li, D. J. Mooney, *Nat. Rev. Mater.* **2016**, *1*, 16071.
[12] P. Dong, B. J. Schott, A. K. Means, M. A. Grunlan, *ACS Appl. Polym. Mater.* **2020**, *2*, 5269.
[13] C. Creton, *Macromolecules* **2017**, *50*, 8297.
[14] M. Najafi, E. Hebels, W. E. Hennink, T. Vermonden, in *Temperature-Responsive Polymers: Chemistry, Properties and Applications* (Eds: V. V. Khutoryanskiy, T. K. Georgiou), Wiley, New York, **2018**, Ch. 1.
[15] U. S. Schubert, H. Hofmeier, G. R. Newkome, *Modern Terpyridine Chemistry*, Wiley-VCH, Weinheim, Germany **2006**.
[16] G. R. Whittell, M. D. Hager, U. S. Schubert, I. Manners, *Nat. Mater.* **2011**, *10*, 176.
[17] M. Shibayama, X. Li, T. Sakai, *Colloid Polym. Sci.* **2019**, *297*, 1.
[18] T. Rossow, S. Seiffert, *Polym. Chem.* **2014**, *5*, 3018.
[19] S. Bode, L. Zedler, F. H. Schacher, B. Dietzek, M. Schmitt, J. Popp, M. D. Hager, U. S. Schubert, *Adv. Mater.* **2013**, *25*, 1634.
[20] M. Sánchez, L. Sabio, N. Gálvez, M. Capdevila, J. M. Dominguez-Vera, *IUBMB Life* **2017**, *69*, 382.
[21] S. Seiffert, W. Oppermann, *J. Microsc.* **2005**, *220*, 20.
[22] G. I. Hauser, S. Seiffert, W. Oppermann, *J. Microsc.* **2008**, *230*, 353.
[23] M. Ahmadi, S. Seiffert, *Soft Matter* **2020**, *16*, 2332.
[24] J. Karvinen, T. O. Ihalainen, M. T. Calejo, I. Jönkkäri, M. Kellomäki, *Mater. Sci. Eng., C* **2019**, *94*, 1056.
[25] S. Hackelbusch, T. Rossow, D. Steinhilber, D. A. Weitz, S. Seiffert, *Adv. Healthcare Mater.* **2015**, *4*, 1841.

 © 2021 The Authors. Macromolecular Chemistry and Physics published by Wiley-VCH GmbH

15213935, 2021, 16, Downloaded from https://onlinelibrary.wiley.com/doi/10.1002/macp.202100076 by Cochrane Germany, Wiley Online Library on [17/10/2022]. See the Terms and Conditions (https://onlinelibrary.wiley.com/terms-and-conditions) on Wiley Online Library for rules of use; OA articles are governed by the applicable Creative Commons License